COUNTING STATISTICS AND ION INTERVAL DENSITY IN AMS

John S Vogel[1] • Ted Ognibene • Magnus Palmblad • Paula Reimer

Center for Accelerator Mass Spectrometry, Lawrence Livermore National Laboratory, Livermore, California 94551, USA.

ABSTRACT. Confidence in the precisions of accelerator mass spectrometry (AMS) and decay measurements must be comparable for the application of the radiocarbon calibration to age determinations using both technologies. We confirmed the random nature of the temporal distribution of ^{14}C ions in an AMS spectrometer for a number of sample counting rates and properties of the sputtering process. The temporal distribution of ion counts was also measured to confirm the applicability of traditional counting statistics.

INTRODUCTION

Accelerator mass spectrometry (AMS) counts radiocarbon and other long-lived isotopes with an efficiency that is many orders of magnitude greater than decay counting. This efficiency leads to precise AMS quantifications of low levels of ^{14}C from small (≤ 1 mg C) and/or old samples. AMS quantification of highly-defined (i.e. small) samples of macrofossils (Kitagawa et al. 1998), corals (Bard et al. 1990), foraminifera (Hughen et al. 1998, 2004; Bard et al. 2004), and stalagmites (Beck et al. 2001) is central to the extension of the ^{14}C calibration and comparisons beyond the dendrochronology of larger tree-ring samples that were quantified by decay counting in establishing Holocene and late-glacial calibrations (Stuiver et al. 1998). Confidence in the precisions of AMS and decay measurements must therefore be comparable for the application of the ^{14}C calibration to age determinations using both technologies. The processes giving rise to individual decay events and mass-separated ion counts are very different, however.

Radioactive decay is known to be a random process of which the decays per counting interval are described by the Poisson distribution (Rutherford and Geiger 1910). The independent nature of each event and the temporal distribution of the decay process are readily understood from the fundamental quantum mechanics of radioactive decay. The randomness of ion arrivals at an AMS counting detector are not as fundamentally obvious, given the complexity of the multiple processes involved in delivery of a specific isotope to the ion counter of an AMS spectrometer. AMS measurements of ^{14}C concentrations arise from negatively ionizing carbon atoms (usually in a sputtering process) from an isolated and chemically prepared sample, followed by mass analysis, acceleration, charge changing by collision electron loss, and identification with counting in an energetic ion detector after mass per charge separation elements. These procedures are not expected to produce temporal correlations within a stream of rare isotopes, and AMS counts should arrive randomly, but their temporal distribution need not mimic that of radioactive decay.

The precision of a random counting measurement is well known to be the square root of the number of independent counts in the measurement. The simple derivation of this concept is in many standard texts and is summarized again by Ogborn et al. (2003). We once more confirmed the random nature of the temporal distribution of ^{14}C ions in an AMS spectrometer for a number of sample counting rates, various sputter energies, and different sample materials. The temporal distribution of ion counts was also inspected to confirm the applicability of traditional counting statistics.

UNCERTAINTIES IN AMS

Soon after the first AMS spectrometers were developed, the quality of AMS measurements was demonstrated through comparisons of the error in the mean of a series of *n* AMS measurements for

---

[1]Corresponding author. Email: jsvogel@llnl.gov.

a sample (external error) to the counting statistics of the measured total counts, *N*, in that series of measurements (internal error). If *μ* is the mean of a group of individual measurements, each with variance σ^2 (here assumed equivalent for all measurements), the fractional precisions were shown to be equivalent to:

$$\sigma_{ext}^2 = \frac{\sigma^2}{n(n-1)\mu^2} = \sigma_{int}^2 = \frac{1}{N_{total}} \qquad (1).$$

Indeed, equivalence of the standard error in the mean of AMS measurements to the precision expected from counting statistics demonstrated the degree to which the spectrometer and its operation are free of systematic error (Wölfli et al. 1983; Donahue et al. 1984; Farwell et al. 1984; Suter et al. 1984). The development of a uniform sample material for ^{14}C AMS, filamentous or fullerene graphite (Vogel et al. 1984), provided intense ion beams for all samples and standards, bringing the internal and external uncertainties into routine equivalence for precise ($\sigma \leq 1\%$) AMS quantification (Bonani et al. 1987; Vogel et al. 1987).

The Lawrence Livermore National Laboratory (LLNL) "compact" spectrometer was designed primarily for biomedical quantifications of ^{14}C and ^{3}H (Ognibene et al. 2002). It contains a 1MV NEC Pelletron accelerator, but was assembled from NEC and LLNL components rather than purchased as a unit. The ion optics of the spectrometer (Ognibene et al. 2000) were designed to accept the output of the LLNL high-intensity ion source (Southon and Roberts 2000), which is routinely operated at ion currents of 100–250 μA ^{12}C$^-$, with ^{14}C count rates of 200–400 cps for Modern samples. These high count rates make possible detailed testing of equivalence between counting statistics and measurement precisions within reasonable time periods. Our isotope ratios are expressed as ^{14}C/^{13}C measured from accelerated ions without corrections for fractionation in preparation.

Figure 1 shows data of multiple measures of an ANU sucrose standard that are completed to a specific number of isotope counts (here $\approx$10,000), providing an expected counting precision of 1% for each measurement. The binned measurements in the histogram to the right in Figure 1 are fit to a normal distribution shown as a line. The Gaussian mean and width fitted to the histogram agree well with the average and standard deviation of the group of 123 measurements (0.9845 ± 0.0092 cts/nC, $\sigma_{dist} = 0.93\%$), in good agreement with the precision of the individual measurements. The uncertainty in the mean of the distribution is $\sigma_{ext} = 0.085\%$, smaller than, but similar to, the expected counting uncertainty due to the total 1,239,000 counts of $\sigma_{int} = 0.090\%$. The top section of the plot compares the cumulative uncertainty due to counting statistics to the cumulative uncertainty in the mean of the measurement series as a function of measurement number. The external error begins larger than the counting statistics but becomes equivalent in less than 10 measurements. The sample was sputtered for over 1 hr and 20 min spread over 4 hr, resulting in a deep "moat" of excavated aluminum around the small fraction of the remaining sample in the holder. Our measurement precision was not affected by this physical modification of the sample.

Biomedical AMS samples, unlike uncontaminated natural ^{14}C samples, often have ^{14}C concentrations greater than Modern, which provided higher count rates for testing equivalences of internal and external uncertainties, as shown in Figure 2. A 5 Modern sample was measured 180 times to show continued equivalence between the two uncertainties to 0.05%. The 5 Modern sample was sputtered for about 1 hr spread over 4 hr, resulting in a deep "pit" in the remaining sample. The constancy of isotope ratio shows that high precision is obtained from fullerene on iron material that is sputtered in a low electric field gradient obtained by recessing the sample surface. Thus, the isotopic fractionations suggested to arise from changes in sample work function and local sample geometry (Nadeau et al. 1987; Nadeau and Litherland 1990) are not present in this ion source from this material to a resolution of 0.05%. The stability of the spectrometer operation over 4 hr was also demonstrated.
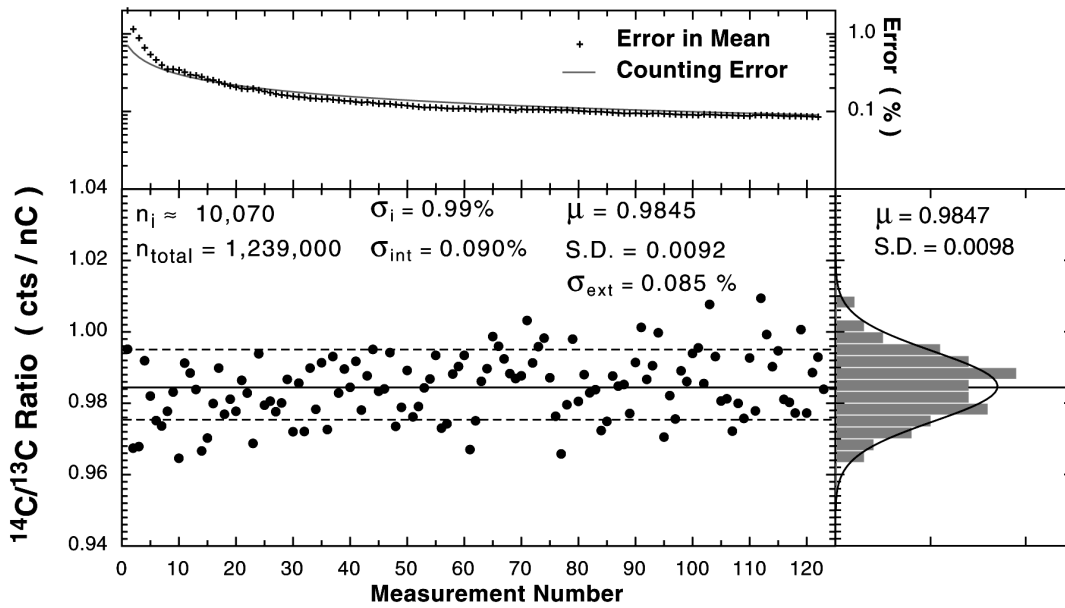
Figure 1 Sequential measurements of a sample of ANU sucrose (1.5 Modern) were distributed normally with a standard deviation equal to the counting statistics of the individual measurements (σ_i). The standard error in the mean of the distribution, $\sigma_{ext} = 0.085\%$, was smaller than the total counting statistics of the entire data set (0.090%).
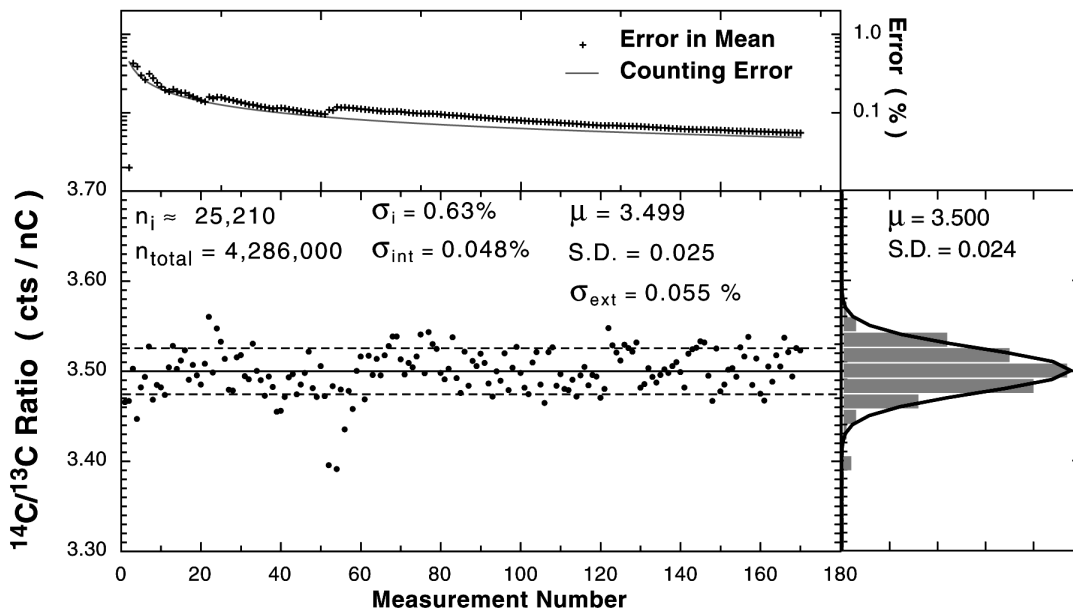

Figure 2 Sequential measurements of a sample of a 5 Modern sample were distributed normally with a standard deviation slightly larger than the counting statistics of the individual measurements (σ_i). The standard error in the mean of the distribution, $\sigma_{ext} = 0.055\%$, was similar to the total counting statistics of the entire data set (0.048%).

DISTRIBUTION OF ION ARRIVAL TIMES

The assumption that AMS ion counts arrive randomly, providing measurements at or near counting statistics, is thus supported through comparable internal and external uncertainties from many laboratories over 20 yr, as well as by the data in the previous section. This random arrival does not necessarily specify the distribution of the ion arrival times in the detector. A recent need to understand our spectrometer live time at very high count rates provided data to determine the distribution of ion arrival times.

We quantified the dependence of the counting live time on the width of the counted pulse using the arrangement outlined in Figure 3. Randomly arriving ^{14}C events striking the solid-state detector were amplified and recognized by a discriminator, the pulse output of which was counted in one channel of a 50-Mhz scalar module in our data acquisition system (Berno et al. 1992). The same pulse triggered a variable width pulser operated in its external trigger mode. The output of this pulser was counted in a second channel of the scalar. This second scalar channel was essentially "dead" to further pulses occurring during its defined pulse width, which was set within 1% accuracy using an oscilloscope. The pulse into the first channel was fixed at 4 µsec. The live time of the second scalar channel was calculated as the ratio of the count rates of the stretched to the parent pulse rates (Ch 2/Ch 1). The "dead" time of the first channel was taken into account in finding the true ion count rates. Our instrumental arrangement creates a "non-extended" dead time in each channel because multiple pulses within the pulse width cannot change the pulse widths.
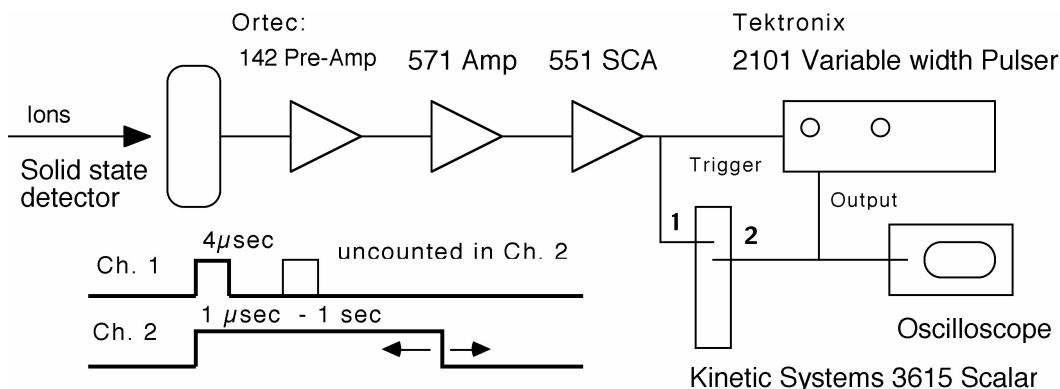
Figure 3 Apparatus for determining the dependence of scalar live time on the ion arrival time distribution

The dependence of live time on pulse width is a function of the distribution of intervals between pulses (the interval density) expressed as multiples of the mean time between ions, hereafter called the "normalized pulse width" (Carloni et al. 1970; Müller 1991). The mean time between ions was determined from the average true count rate during each scalar acquisition, which normalized the data for changes in ion source output and permitted comparisons among different count rates. The live time of channel 2 was found for pulse widths from a microsecond to a second, corresponding to 6 orders of magnitudes in the normalized pulse widths.

A wide range of ^{14}C concentrations were available from an assortment of biological samples ranging from 0.1 to 200 Modern for these tests. The sample materials were our usual fullerene on iron/cobalt catalyst (Vogel et al. 1984; Vogel 1992; Ognibene et al. 2003). Cathode potential is a convenient control of count rate from our ion source because we do not see a marked change in ion transmission

or isotope ratio, despite the large changes available in emitted beam intensity. We use this capability to reduce the count rate from samples having unexpectedly high ^{14}C levels in biological studies. We varied the cathode potential over our usual operating range (3 kV to 10 kV) to reveal any changes in the ion arrival distribution due to sputtering energy, which also affects temperature of the sample through the power deposited by the cesium. We selected samples for each of 3 cathode potentials that produced equivalent count rates of ≈700 counts per second (Bq). The live time of the widened pulse scalar is shown as a function of the normalized pulse width for 3-, 5-, and 10-kV cathode potentials in Figure 3a. The data are indistinguishable for each condition. Monte Carlo simulations of the experimental arrangement assumed normal, log normal, and Poisson probability distributions for the ion count rate distribution. The data show an excellent fit to the live time predicted by an exponential arrival distribution indicative of a Poisson process, while the normal and log-normal distributions of count rates overpredict the live times for widths less than the mean times between events.

The scalar live time was also determined as a function of scalar pulse widths for counting rates differing by a factor of 4000 using different samples sputtered at a single cesium energy (8 kV), shown in Figure 4b. All live times were identical at equivalent normalized pulse widths, showing that interval densities were described by a single parameter, the mean counting rate, as expected for a Poisson process. A Poisson process has 3 characteristics: the number of events in non-overlapping intervals are independent; intervals can be made small enough to contain only 1 event; and the probability of an event occurring in an interval is independent of the interval's starting time. From this definition, an exponential form for the arrival density is derived with a dependence on count rate. A Poisson distribution for rate measurements results (Carloni et al. 1970). The live time for our non-extended triggers takes the form (Müller 1991):

$$Live \ = \ \frac{R_{meas}}{R_{true}} \ = \ \frac{1}{(1 + \tau \times R_{true})} \ = \ \frac{1}{(1 + NPW)} \tag{2},$$

where R is the measured or true ion rate, τ is the fixed width of a counted pulse, and *NPW* is a normalized pulse width of the counted pulse. A nonlinear regression of all data to this relation has a r^2 of 0.99997 with a standard deviation of the residuals equal to 0.3%.

The Poisson distribution describes the results of a large number of trials of an improbable event. In this case, the probability of emission of a ^{14}C is low amid the large number (>10^{12} greater) of ions emitted from the sputtered sample under the intense bombardment of cesium ions. This is the likely source of the Poisson nature of AMS counts. If the Poisson nature of the count arrival times is not a surprise, the purity of its fit to the data is telling. The presence of any other process in the entire AMS system that was of a similar low probability would skew the Poisson distribution. This also holds true for the multiple components of the sputtering process itself, including collisional release of the ion, its acceptance of an electron at the sample surface, and its survival against collisional or electrical charge neutralization. All other processes must have large probabilities of ion survival compared to the Poisson behavior of the collisional emittance of a ^{14}C from the sample.

CONCLUSION

We showed experimentally that the long-assumed Poisson nature of AMS counts holds over a wide range of count rates under varying source conditions. The purity of the Poisson distribution shows that there are no fundamental limits placed on the ultimate counting precision attainable by AMS. We demonstrated that very low count rate samples also follow the Poisson distribution, showing that AMS measurements of very old materials may be used in generating calibration data with their precision reflected in the stated counting statistics.
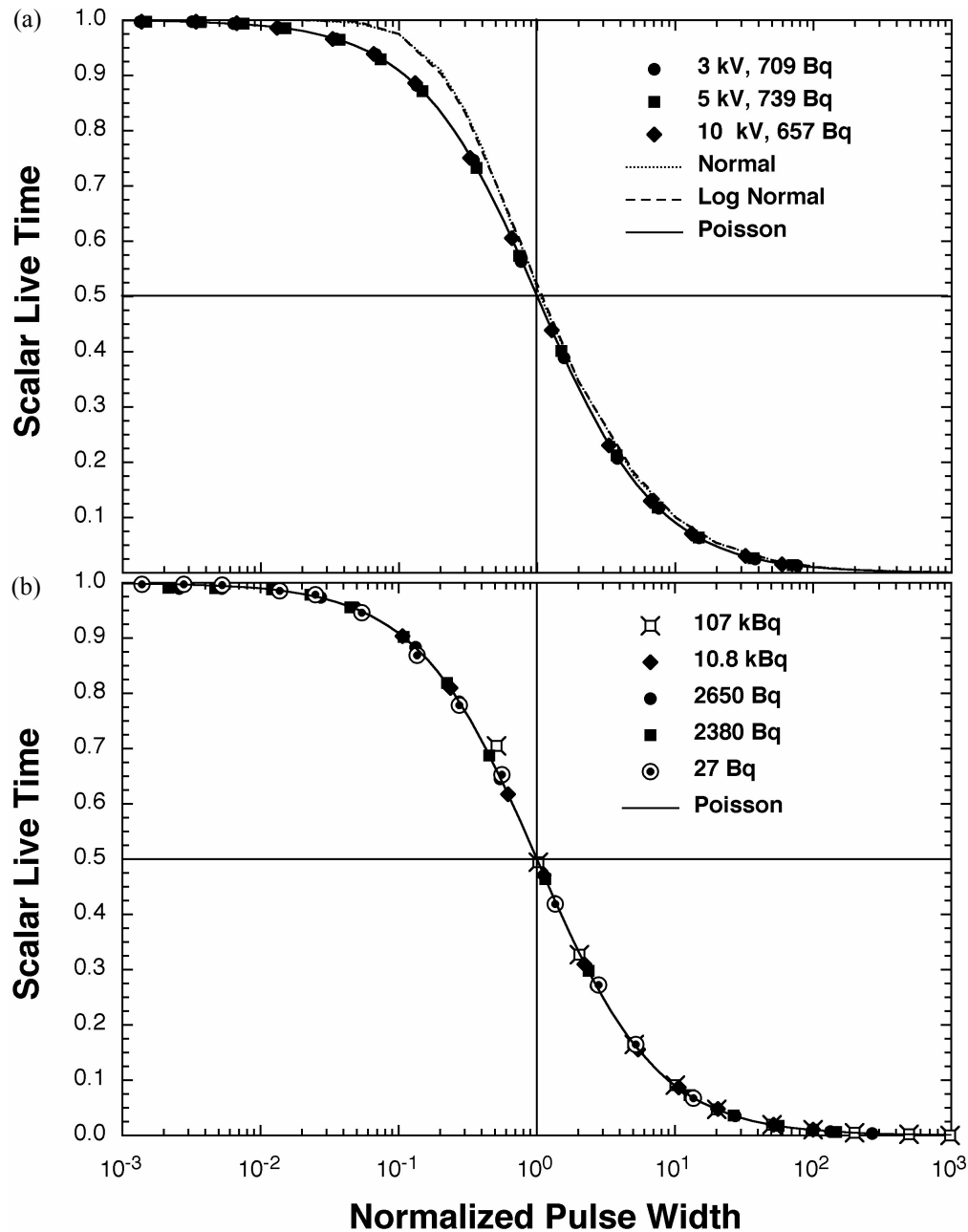
(a)

(b)

Figure 4 (a) The scalar live time follows the same function of normalized pulse width for 3 different cesium sputtering energies. The function is best described by a Monte Carlo simulation assuming a Poisson distribution of ion arrival times; (b) The same function of live time is found for a range of mean count rates from 27 to 107,000 counts per second.

ACKNOWLEDGMENTS

REFERENCES

Bard E, Hamelin B, Fairbanks RG, Zindler A. 1990. Calibration of the ^{14}C time scale over the past 30,000 years using mass spectrometric U-Th ages from the Barbados corals. *Nature* 345:405–10.

Bard E, Rostek F, Ménot-Combes G. 2004. Radiocarbon calibration beyond 20,000 ^{14}C yr BP by means of planktonic foraminifera of the Iberian Margin. *Quaternary Research* 61:204–14.

Beck JW, Richards DA, Edwards RL, Silverman BW, Smart PL, Donahue DJ, Hererra-Osterheld S, Burr GS, Calsoyas L, Jull AJT, Biddulph D. 2001. Extremely large variations of atmospheric ^{14}C concentration during the last glacial period. *Science* 292: 2453–8.

Berno AJ, Vogel JS, Caffee M. 1991. High-speed data acquisition of multi-parameter data using a Macintosh IIcx. *Nuclear Instruments and Methods in Physics Research B* 56:1076–9.

Bonani G, Beer J, Hofmann H, Synal H-A, Suter M, Wölfli W, Pfleiderer C, Kromer B, Junghans C, Münnich KO. 1987. Fractionation, precision and accuracy in ^{14}C and ^{13}C measurements. *Nuclear Instruments and Methods in Physics Research B* 29:87–90.

Buchholz BA, Freeman SPHT, Haack KW, Vogel JS. 2000. Tips and traps in the ^{14}C bio-AMS preparation laboratory. *Nuclear Instruments and Methods in Physics Research B* 172:404–8.

Carloni F, Corberi A, Marseguerra M, Porceddu CM. 1970. The asymptotic method of dead time correction in Poissania distribution. *Nuclear Instruments and Methods in Physics Research B* 78:70–6.

Donahue D, Jull AJT, Zabel TH. 1984. Results of radioisotope measurements at NSF-University of Arizona tandem accelerator mass spectrometry facility. *Nuclear Instruments and Methods in Physics Research B* 5:162–6.

Farwell GW, Grootes PM, Leach DD, Schmidt FH. 1984. The accelerator mass spectrometry facility at the University of Washington: current status and application to a ^{14}C profile of a tree ring. *Nuclear Instruments and Methods in Physics Research B* 5:144–9.

Hughen KA, Overpeck JT, Lehman SJ, Kashgarian M, Southon JR, Peterson LC, Alley R, Sigman DM. 1998. Deglacial changes in ocean circulation from an extended radiocarbon calibration. *Nature* 391:65–8.

Hughen KA, Lehman S, Southon J, Overpeck J, Marchal O, Herring C, Turnbull J. 2004. ^{14}C activity and global carbon cycle changes over the past 50,000 years. *Science* 303:202–7.

Kitagawa H, van der Plicht J. 1998. Atmospheric radiocarbon calibration to 45,000 yr BP—Late Glacial fluctuations and cosmogenic isotope production. *Science* 279:1187–90.

Müller JW. 1991. Generalized dead times. *Nuclear Instruments and Methods in Physics Research A* 301: 543–51.

Nadeau MJ, Kieser WE, Buekens RP, Litherland AE. 1987. Quantum mechanical effects on sputter source isotope fractionation. *Nuclear Instruments and Methods in Physics Research B* 29:83–6.

Nadeau MJ, Litherland AE. 1990. Electric dissociation of negative ions. *Nuclear Instruments and Methods in Physics Research B* 52:387–90.

Ogborne J, Collins S, Brown M. 2003. Randomness at the root of things: random walks. *Physics Education* 38:391–7.

Ognibene TJ, Brown TA, Knezovich JP, Roberts ML, Southon JR, Vogel JS. 2000. Ion-optics calculations of the LLNL AMS system for biochemical ^{14}C measurements. *Nuclear Instruments and Methods in Physics Research B* 172:47–51.

Ognibene TJ, Bench G, Brown TA, Peaslee GF, Vogel JS. 2002. A new accelerator mass spectrometry system for ^{14}C-quantification of biochemical samples. *Journal of Mass Spectrometry and Ion Processes* 218:255–64.

Ognibene TJ, Bench G, Vogel JS, Peaslee GF, Murov S. 2003. A high-throughput method for the conversion of CO_2 obtained from biochemical samples to graphite in septa-sealed vials for quantification of ^{14}C via accelerator mass spectrometry. *Analytical Chemistry* 75: 2192–6.

Rutherford E, Geiger H. 1910. The probability variations in the distribution of alpha-particles. *Philosophical Magazine* 20:698–707.

Southon JR, Roberts ML. 2000. Ten years of sourcery at CAMS/LLNL: evolution of a Cs ion source. *Nuclear Instruments and Methods in Physics Research B* 172: 257–61.

Suter M, Balzer R, Bonani G, Hofmann H, Morenzoni E, Nessi M, Wölfli W, Andreé M, Beer J, Oeschger H. 1984. Precision measurements of ^{14}C in AMS—some results and prospects. *Nuclear Instruments and Methods in Physics Research B* 5:117–22.

Vogel JS, Southon JR, Nelson DE, Brown TA. 1984. Performance of catalytically condensed carbon for use in accelerator mass spectrometry. *Nuclear Instruments and Methods in Physics Research B* 5:289–93.

Vogel JS, Southon JR, Nelson DE. 1987. Catalyst and binder effects in the use of filamentous graphite for AMS. *Nuclear Instruments and Methods in Physics Research B* 29:50–6.

Vogel JS. 1992. Rapid production of graphite without contamination for biomedical AMS. *Radiocarbon* 34(3):344–50.

Wölfli W, Bonani G, Suter M, Balzer R, Nessie M, Stoller C, Beer J, Oeschger H, Andreé M. 1983. Radioisotope dating with the ETHZ EN tandem accelerator. *Radiocarbon* 25(2):745–54.